JACS
JOURNAL OF THE AMERICAN CHEMICAL SOCIETY
Communication
pubs.acs.org/JACS

Extreme Conductance Suppression in Molecular Siloxanes

Haixing Li,[⊥,†] Marc H. Garner,[⊥,‡] Timothy A. Su,[⊥,§] Anders Jensen,[‡] Michael S. Inkpen,[†] Michael L. Steigerwald,[*,§] Latha Venkataraman,[*,†,§] Gemma C. Solomon,[*,‡] and Colin Nuckolls[*,§]

[†]Department of Applied Physics and Applied Mathematics, Columbia University, New York, New York 10027, United States
[‡]Nano-Science Center and Department of Chemistry, University of Copenhagen, Universitetsparken 5, 2100 Copenhagen Ø, Denmark
[§]Department of Chemistry, Columbia University, New York, New York 10027, United States

Supporting Information

ABSTRACT: Single-molecule conductance studies have traditionally focused on creating highly conducting molecular wires. However, progress in nanoscale electronics demands insulators just as it needs conductors. Here we describe the single-molecule length-dependent conductance properties of the classic silicon dioxide insulator. We synthesize molecular wires consisting of Si−O repeat units and measure their conductance through the scanning tunneling microscope-based break-junction method. These molecules yield conductance lower than alkanes of the same length and the largest length-dependent conductance decay of any molecular systems measured to date. We calculate single-molecule junction transmission and the complex band structure of the infinite 1D material for siloxane, in comparison with silane and alkane, and show that the large conductance decay is intrinsic to the nature of the Si−O bond. This work highlights the potential for siloxanes to function as molecular insulators in electronics.

Silicon dioxide is a critical dielectric material in electronics;[1] polysiloxanes display ideal properties for use in flexible polymer transistors.[2,3] Organic molecular materials containing Si−O bonds have been shown to be promising dielectrics for organic field-effect transistors,[4,5] particularly as insulating thin-films in dielectric organic−inorganic hybrid materials.[6] The electronic structure of SiO_2[7,8] and the electronic characteristics of the Si−O bonds in siloxanes has been addressed in the literature.[9,10] On the molecular scale, the impact of oxygen heteroatoms on the transport capability of alkane wires has been investigated.[11−14] However, despite the ubiquitous use of materials containing Si−O bonds in electronics, the charge transport properties of Si−O bonds at the single molecule level have received little attention. Although most of the emphasis in molecular electronics has been placed on developing conducting, switching or rectifying molecular wires, the development of high-performing molecular insulators has been neglected. These molecular insulators will serve a complementary role in arrays of molecular electronic components, as they will serve to prevent electronic cross-talk between molecular conductors within the array. Furthermore, in developing functional single-molecule components such as transistors or switches, insulators are of use when active molecular electronic components need to be decoupled from electrodes (i.e., Coulomb blockade effects).[15]

Here we synthesize a series of dimethylsiloxane oligomers terminated with aurophilic methylthiomethyl electrode-linking groups. Using the scanning tunneling microscope break junction technique (STM-BJ),[16,17] we create single molecule circuits with these siloxane molecular wires and measure their conductance. These oligo(dimethylsiloxane) wires demonstrate the highest conductance decay measured to date, highlighting their strong insulator characteristics. We compare these new materials with previously studied silanes and alkanes experimentally as well as computationally through density functional theory (DFT) calculations. Complex band structure analysis of the infinite 1D chains of siloxane, silane, and alkane further illustrates that despite the larger band gap of the alkane chain, the siloxane chain shows larger conductance decay. We find that the weak electronic coupling across the siloxane wire arises from the highly polarized nature of the Si−O bond.

The oligo(dimethylsiloxane)s **1−3** were synthesized (Scheme 1) by reacting the previously reported methylthio-

Scheme 1. Synthesis of 1−3

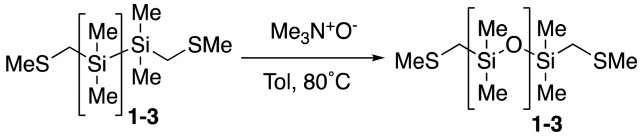

methyl-terminated permethyloligosilanes with trimethylamine *N*-oxide (detailed synthetic procedures given in Supporting Information, Section I).[18] The synthesis of 1,12-bis(methylthio)dodecane is provided in SI, Section I;[19] the synthesis and measurements of linear silanes and alkanes were reported previously.[20,21] We measured the oligo(dimethylsiloxane)s (Figure 1a) using the STM-BJ as follows. We repeatedly bring the Au STM tip in and out of contact with an Au substrate in a solution of the target molecule while recording the junction conductance. Once the contact between the tip and the substrate ruptures, a molecule can bridge the gap and form a single molecule junction.

We collect thousands of such conductance-versus-displacement traces and generate the 1D log-binned conductance

Received: May 30, 2017
Published: July 13, 2017

DOI: 10.1021/jacs.7b05599
J. Am. Chem. Soc. 2017, 139, 10212−10215

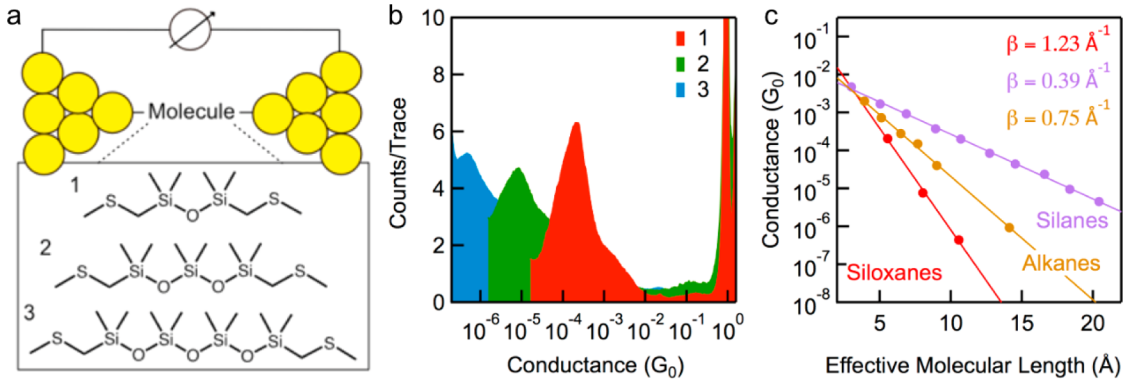

Figure 1. (a) Schematic representation of a molecular junction showing the structures of siloxanes **1**−**3**. (b) 1D log-binned conductance histograms compiled from more than 10 000 traces without any data selection for **1**−**3** measured in 1,2,4 trichlorobenzene at a bias of ∼0.2, 0.5, and 1.8 V respectively. (c) Plot of the conductance as a function of the effective molecular length, defined as the distance between the two distal methylenes in each DFT-optimized structure, for **1**−**3** in comparison with linear silanes and alkanes (molecular structures see SI Figure S1; conductance histograms for alkanes are provided in SI Figure S2). Using $G = G_c e^{-\beta L}$, we determine a decay constant of 1.23 ± 0.05 Å^{-1} for siloxanes, 0.39 ± 0.01 Å^{-1} for silanes, and 0.75 ± 0.02 Å^{-1} for alkanes.

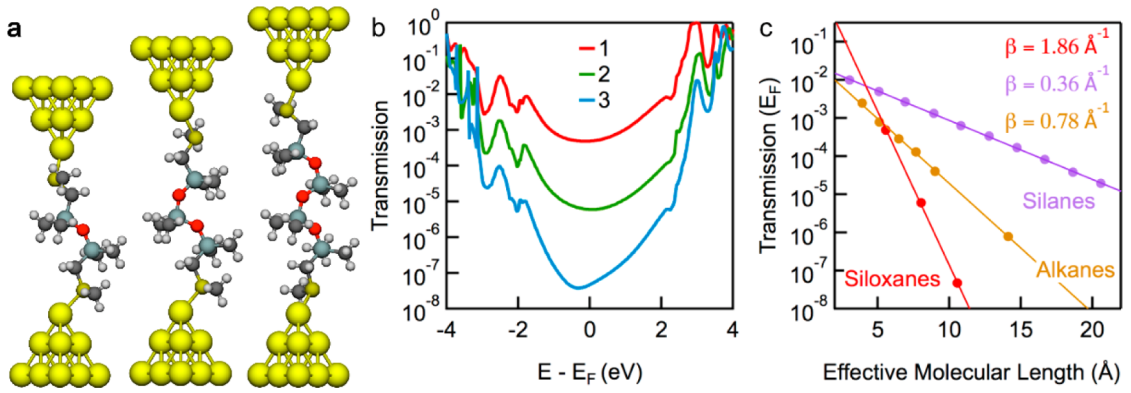

Figure 2. (a) Optimized junction geometry and (b) calculated transmission curves of **1**−**3**. (c) Plot of calculated transmissions at the Fermi energy as a function of the effective molecular length for **1**−**3** in comparison with linear silanes and alkanes. Using $G = G_c e^{-\beta L}$, we determine a decay constant of 1.86 ± 0.04 Å^{-1} for siloxanes, 0.36 ± 0.002 Å^{-1} for silanes, and 0.78 ± 0.01 Å^{-1} for alkanes.

histograms shown in Figure 1b without any data selection. We observe conductance peaks at integer multiples of $G_0 = 2e^2/h$, the quantum of conductance, and at a molecule dependent value below $1G_0$ due to the formation of a single molecule junction. We determine the molecular conductance by fitting a Gaussian function to the conductance peak and plot the peak values on a semilogarithmic scale against the effective molecular length. The exponential decay of conductance with increasing length $G = G_c e^{-\beta L}$ is clearly seen in Figure 1c. When the siloxanes are compared with alkanes of the same length, their conductance is lower in all the systems measured. The decay constant β = 1.23 ± 0.05 Å^{-1} for siloxanes is 3 times that of linear silanes (0.39 Å^{-1}).[20] Moreover, the decay constant for the siloxanes is significantly higher than that of alkanes (0.74 Å^{-1}), which are often considered the prototypical molecular insulator.

For more insight into the steep conductance decay in siloxanes, we carried out calculations with DFT and the nonequilibrium Green's functions (NEGF) formalism.[22] First, we analyze conformations that may contribute to the molecular conductance. We optimize the molecular structures to a force threshold of 0.01 eV Å^{-1} using DFT with the Perdew−Burke−Ernzerhof exchange−correlation (PBE-XC) functional[23] and double-ζ plus polarization basis set as implemented in projector-augmented wave code within the Atomic Simulation Environment (ASE/GPAW).[24,25] In agreement with previous studies, we find that siloxanes are very flexible molecules and the energy differences between conformations are small.[9,10,26,27] We therefore focus here on the longest conformations of each siloxane (more details on the effect of conformation on transmission are given in SI part III B, C). We attach gold electrodes, which are composed of two 4-atom Au-pyramids placed on a 4 × 4 fcc Au(111) surface to the relaxed molecular structures to form junctions (Figure 2a). The molecule is further relaxed to 0.05 eV Å^{-1} while keeping the Au-atoms fixed. Finally, we calculate the Landauer transmission through the junction.

The calculated transmissions are shown on a semilogarithmic scale against energy in Figure 2b (silanes and alkanes data are shown in SI Figure S3 and S4). We find that the transmission values close to the Fermi energy are drastically reduced with increasing molecular length. We plot transmission value at E_F for each molecule against the effective molecular length in Figure 2c. The calculated transmission shows the steepest conductance decay for siloxanes and the shallowest for silanes, in good agreement with the experimental findings. We note that, for the siloxane, β is overestimated in the theoretical results compared with what is observed experimentally. This could, in part, be due to the errors inherent to DFT calculations, which likely explains the strong energy depend-

DOI: 10.1021/jacs.7b05599
J. Am. Chem. Soc. 2017, 139, 10212−10215

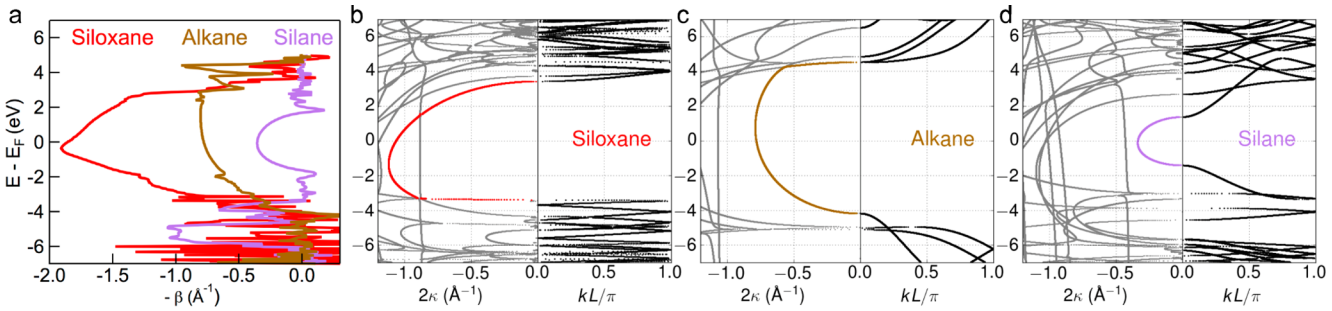

Figure 3. (a) Conductance decay parameter β from the transmission calculations plotted versus the Fermi energy of gold. (b–d) Complex band structure for siloxane, silane, and alkane 1D nanowires plotted versus the Fermi energy of the respective systems. On the right-hand side of the plot, the real bands are plotted with the purely real k. On the left-hand side, 2 times the imaginary part of the complex wave vector 2κ is plotted. Note the relationship $\beta = 2\kappa$. The colored complex band indicates the band with (expected) largest contribution to the transmission.

ence of β (Figure 3a).[28] However, it could also be due to the difference between the length of the junction sampled in the experiments when compared to the DFT-based backbone length. Indeed, we find that if we plot the measured conductance versus the measured junction elongation length, as shown in Figure S5, the siloxane β increases to 1.45 ± 0.04 Å^{-1}, closer to the calculated value.

The shallow conductance decay of silanes is closely linked to the relatively strong electronic coupling through their backbones, which is a consequence of the well-studied σ-conjugation effect.[29,30] Indeed, the gap between the highest occupied molecular orbital (HOMO) and the lowest unoccupied molecular orbital (LUMO) of silanes become smaller with increasing length.[31] On the other hand, for the alkanes and siloxanes, the calculated HOMO–LUMO gaps are essentially length independent, indicating that the electronic coupling across the backbone is very weak (see Table S1 in SI part III D).

The transmission and electronic structure calculations for **1**–**3** strongly agree with the experimental finding that Si–O bonds suppress the conductance. To probe the physical origin of this suppression, we model the complex band structure of the infinite 1D chains of siloxane, silane, and alkane. In this type of calculation, the electronic structure of the molecular backbone is isolated from effects relating to the conformational freedom and the binding groups of the molecules. The complex band structure describes the decay of the tunneling/local states inside the band gap and the imaginary part of the wave vector (κ) is directly related to conductance decay constant through $\beta = 2\kappa$, given only one contributing channel.[32,33] We calculate the complex band structure by optimizing the unit cell for infinite periodic chains of $[-SiMe_2-O-SiMe_2-O-]_n$, $[-SiMe_2-SiMe_2-]_n$, and $[-CH_2-CH_2-]_n$ using the same methods detailed above with the Atomistix ToolKit software.[34] See SI part III E for further details.

Figure 3b–d shows the complex bands for the siloxane-, alkane-, and silane-based 1D chains; the colored regions of the complex bands, determined by comparing these to Figure 3a, are expected to dominate transport. Our key finding here is that the band gap does not predict β. The band gap for siloxane, which has a larger β, is ∼6 eV, whereas that of the alkane is ∼8 eV. It appears that the dispersion in the real bands (right-hand side of each plot) can be related to the curvature of the complex bands and thus β. The most striking feature in the band structure of the siloxane is the prevalence of relatively flat bands. This can be attributed to strong polarity of the Si–O bond due to the very different electronegativities of Si and O, when compared with either the C–C bond or Si–Si bond. This polarity leads to charge localization and flat bands (indicating weak electronic coupling through the material) and translates into a deep valley in the complex band near the Fermi energy. In contrast with the fast decay of siloxane and alkane, the silane chain in Figure 3c has a narrow band gap ∼2 eV, high dispersion, and consequently a small decay constant. The alkane forms an intermediate case. The discrepancies between the energy dependent β as shown in Figure 3a and dominant complex bands in Figure 3b–d are expected when considering interface effects, the addition of binding groups, and the difference in Fermi energy.

To conclude, the siloxane molecular wires measured here demonstrate the largest length-dependent conductance decay observed to date. The large conductance decay factor of siloxanes is not a consequence of the HOMO–LUMO gap or the conformational freedom of the molecule, but rather the electronic structure of the molecular backbone, which effectively promotes charge localization. The agreement between our complex band structure calculations and the single-molecule conductance experiments suggest that these atomic-size siloxane wires allow us to nonetheless probe the polymeric limit of this material. Such a capability to capture the electronic trends from small siloxanes highlights the special nature of the Si–O bond. Our results imply that from the smallest siloxane molecule to bulk SiO_2, this bonding motif effectively suppresses electronic coupling without compromising structural stability. Though SiO_2 has repeatedly proven its utility as an insulator and dielectric material, these results reveal the prospects of siloxanes to achieve these same functions on the molecular scale. The superior charge insulating properties of the siloxane chains studied here suggests that they can serve as improved replacements of the alkanes typically used for decoupling the central unit from the electrode in molecular devices.

■ ASSOCIATED CONTENT

Supporting Information

The Supporting Information is available free of charge on the ACS Publications website at DOI: 10.1021/jacs.7b05599.

Additional figures, synthetic details, characterization data, STM-BJ experimental details, and DFT calculation details (PDF)

DOI: 10.1021/jacs.7b05599
J. Am. Chem. Soc. 2017, 139, 10212–10215

AUTHOR INFORMATION

Corresponding Authors

*mls2064@columbia.edu
*lv2117@columbia.edu
*gsolomon@chem.ku.dk
*cn37@columbia.edu

ORCID

Haixing Li: 0000-0002-1383-4907
Marc H. Garner: 0000-0002-7270-8353
Timothy A. Su: 0000-0001-5934-3292
Latha Venkataraman: 0000-0002-6957-6089
Gemma C. Solomon: 0000-0002-2018-1529
Colin Nuckolls: 0000-0002-0384-5493

Present Address

T.A.S.: Department of Chemistry, University of California, Berkeley, Berkeley, CA 94720, United States

Author Contributions

⊥H.L., M.H.G., and T.A.S. contributed equally.

Notes

The authors declare no competing financial interest.

ACKNOWLEDGMENTS

We thank Prof. Luis Campos for helpful discussions and for providing synthetic laboratory equipment. We acknowledge Dr. Brandon Fowler for mass spectrometry characterization. We thank NSF for support of experimental studies under grant no. CHE-1404922 (H.L.). G.C.S., M.H.G., and A.J. received funding from the Danish Council for Independent Research Natural Sciences and the Carlsberg Foundation. T.A.S. was supported by the NSF Graduate Research Fellowship under grant no. 11-44155. M.S.I. was supported primarily by a Marie Skłodowska Curie Global Fellowship (M.S.I., MOLCLICK: 657247) within the Horizon 2020 Programme.

REFERENCES

(1) Kingon, A. I.; Maria, J.-P.; Streiffer, S. K. *Nature* **2000**, *406*, 1032−1038.
(2) Schwartz, G.; Tee, B. C. K.; Mei, J.; Appleton, A. L.; Kim, D. H.; Wang, H.; Bao, Z. *Nat. Commun.* **2013**, *4*, 1859.
(3) Akogwu, O.; Kwabi, D.; Munhutu, A.; Tong, T.; Soboyejo, W. O. *J. Appl. Phys.* **2010**, *108*, 123509.
(4) Chua, L.-L.; Zaumseil, J.; Chang, J.-F.; Ou, E. C. W.; Ho, P. K. H.; Sirringhaus, H.; Friend, R. H. *Nature* **2005**, *434*, 194−199.
(5) Yoon, M.-H.; Facchetti, A.; Marks, T. J. *Proc. Natl. Acad. Sci. U. S. A.* **2005**, *102*, 4678−4682.
(6) Ha, Y.-G.; Everaerts, K.; Hersam, M. C.; Marks, T. J. *Acc. Chem. Res.* **2014**, *47*, 1019−1028.
(7) Stixrude, L.; Devine, R.; Duraud, J.; Dooryhée, E. *Structure and imperfections in amorphous and crystalline silicon dioxide*; Wiley: Chichester, England, 2000.
(8) Binggeli, N.; Troullier, N.; Martins, J. L.; Chelikowsky, J. R. *Phys. Rev. B: Condens. Matter Mater. Phys.* **1991**, *44*, 4771−4777.
(9) Weinhold, F.; West, R. *Organometallics* **2011**, *30*, 5815−5824.
(10) Weinhold, F.; West, R. *J. Am. Chem. Soc.* **2013**, *135*, 5762−5767.
(11) Napper, A. M.; Liu, H.; Waldeck, D. H. *J. Phys. Chem. B* **2001**, *105*, 7699−7707.
(12) Wierzbinski, E.; Yin, X.; Werling, K.; Waldeck, D. H. *J. Phys. Chem. B* **2013**, *117*, 4431−4441.
(13) Xie, Z.; Bâldea, I.; Oram, S.; Smith, C. E.; Frisbie, C. D. *ACS Nano* **2017**, *11*, 569−578.
(14) Baghbanzadeh, M.; Bowers, C. M.; Rappoport, D.; Żaba, T.; Yuan, L.; Kang, K.; Liao, K.-C.; Gonidec, M.; Rothemund, P.; Cyganik, P.; Aspuru-Guzik, A.; Whitesides, G. M. *J. Am. Chem. Soc.* **2017**, *139*, 7624−7631.
(15) Su, T. A.; Neupane, M.; Steigerwald, M. L.; Venkataraman, L.; Nuckolls, C. *Nat. Rev. Mater.* **2016**, *1*, 16002.
(16) Xu, B.; Tao, N. J. *Science* **2003**, *301*, 1221−1223.
(17) Venkataraman, L.; Klare, J. E.; Tam, I. W.; Nuckolls, C.; Hybertsen, M. S.; Steigerwald, M. L. *Nano Lett.* **2006**, *6*, 458−462.
(18) Sakurai, H.; Hirama, K.; Nakadaira, Y.; Kabuto, C. *J. Am. Chem. Soc.* **1987**, *109*, 6880−6881.
(19) Su, T. A.; Li, H.; Zhang, V.; Neupane, M.; Batra, A.; Klausen, R. S.; Kumar, B.; Steigerwald, M. L.; Venkataraman, L.; Nuckolls, C. *J. Am. Chem. Soc.* **2015**, *137*, 12400−12405.
(20) Su, T. A.; Li, H.; Steigerwald, M. L.; Venkataraman, L.; Nuckolls, C. *Nat. Chem.* **2015**, *7*, 215−220.
(21) Park, Y. S.; Whalley, A. C.; Kamenetska, M.; Steigerwald, M. L.; Hybertsen, M. S.; Nuckolls, C.; Venkataraman, L. *J. Am. Chem. Soc.* **2007**, *129*, 15768−15769.
(22) Chen, J. Z.; Thygesen, K. S.; Jacobsen, K. W. *Phys. Rev. B: Condens. Matter Mater. Phys.* **2012**, *85*, 155140.
(23) Perdew, J. P.; Burke, K.; Ernzerhof, M. *Phys. Rev. Lett.* **1996**, *77*, 3865−3868.
(24) Bahn, S. R.; Jacobsen, K. W. *Comput. Sci. Eng.* **2002**, *4*, 56−66.
(25) Mortensen, J. J.; Hansen, L. B.; Jacobsen, K. W. *Phys. Rev. B: Condens. Matter Mater. Phys.* **2005**, *71*, 035109.
(26) Al Derzi, A. R.; Gregušová, A.; Runge, K.; Bartlett, R. J. *Int. J. Quantum Chem.* **2008**, *108*, 2088−2096.
(27) Moraru, I.-T.; Petrar, P. M.; Nemeş, G. *J. Phys. Chem. A* **2017**, *121*, 2515−2522.
(28) Tamblyn, I.; Darancet, P.; Quek, S. Y.; Bonev, S. A.; Neaton, J. B. *Phys. Rev. B: Condens. Matter Mater. Phys.* **2011**, *84*, 84.
(29) Bande, A.; Michl, J. *Chem. - Eur. J.* **2009**, *15*, 8504−8517.
(30) Schepers, T.; Michl, J. *J. Phys. Org. Chem.* **2002**, *15*, 490−498.
(31) Tsuji, H.; Terada, M.; Toshimitsu, A.; Tamao, K. *J. Am. Chem. Soc.* **2003**, *125*, 7486−7487.
(32) Tomfohr, J. K.; Sankey, O. F. *Phys. Rev. B: Condens. Matter Mater. Phys.* **2002**, *65*, 245105.
(33) Jensen, A.; Smidstrup, S.; Stockbro, K.; Solomon, G. C.; Reuther, M. G. Complex band structure and electronic transmission, submitted.
(34) *Atomistix ToolKit QuantumWise A/S*, version 2016.3 (http://www.quantumwise.com).

DOI: 10.1021/jacs.7b05599
J. Am. Chem. Soc. 2017, 139, 10212−10215